

mer, J. I. Mills, and R. A. Day, *J. Quant. Spectrosc. Radiat. Transfer* **10**, 629 (1970).

⁹J. D. Jackson, *J. Nucl. Energy, Part C* **1**, 171 (1960).

¹⁰H. Tanaka, A. Hirose, and M. Koganei, *Phys. Rev.* **161**, 94 (1967).

¹¹R. Z. Sagdeev and A. A. Galeev, *Nonlinear Plasma Theory*, edited by T. M. O'Neil and D. L. Book (Benjamin, New York, 1969), p. 103.

¹²V. L. Sizonenko and K. N. Stepanov, *Pis'ma Zh. Eksp. Teor. Fiz.* **9**, 468 (1969) [*JETP Lett.* **9**, 282 (1969)].

¹³B. A. Demidov, N. I. Elagin, and S. D. Fanchenko,

Dokl. Akad. Nauk SSSR **174**, 327 (1967) [*Sov. Phys. Dokl.* **12**, 467 (1967)].

¹⁴E. E. Field and B. D. Fried, *Phys. Fluids* **7**, 1937 (1964).

¹⁵G. A. Bovrovskii, A. I. Kislyakov, M. P. Petrov, K. A. Razumova, and D. A. Shcheglov, in *Proceedings of the International Symposium on Closed Confinement Systems*, Dubna, U. S. S. R., 29 September–3 October 1969 (unpublished).

¹⁶A. W. Trivelpiece, *Slow Wave Propagation in Plasma Waveguides* (San Francisco Press, Inc., San Francisco, Calif., 1967).

Evolution and Large-Electric-Field Suppression of the Transverse Kelvin-Helmholtz Instability

D. L. Jassby*

Plasma Physics Laboratory, Princeton University, Princeton, New Jersey 08540

(Received 14 September 1970)

The interior of a plasma column is subjected to shear of arbitrary magnitude in the $\vec{E} \times \vec{B}$ rotation. The resultant Kelvin-Helmholtz instability undergoes an evolution in mode structure as the radial electric field is increased, and is suppressed when the Doppler-shifted wave frequency equals 0.5 to 0.65 times the ion-cyclotron frequency. Cyclotron waves appear concomitant with this suppression; these have properties in agreement with linear fluid theory.

A cylindrical plasma column in a uniform axial magnetic field and a nonuniform radial electric field is unstable to Kelvin-Helmholtz waves if the shear in the $\vec{E} \times \vec{B}$ rotation is sufficiently large. For example, the edge oscillation of *Q* machines is essentially a transverse Kelvin-Helmholtz instability.^{1,2} In order to study this instability in detail, we have set up a velocity shear layer of externally controlled magnitude. In this Letter we describe how the observed instability evolves as the radial electric field is increased from zero to large values.

The significant experimental results, at large electric field, are the suppression of the low-frequency instability when the Doppler-shifted wave frequency is slightly greater than one-half the ion-cyclotron frequency ω_c and, concomitant with this suppression, the appearance of coherent, higher-frequency oscillations near ω_c . A radial wave equation valid for instabilities of arbitrary frequency in a nonuniformly rotating plasma cylinder is presented. This equation has two sets of solutions: One set corresponds to the observed high-frequency modes near ω_c ; the other set consists of the low-frequency Kelvin-Helmholtz modes. The suppression of the low-frequency waves occurs at the resonant condition

for nonlinear Landau damping.³

The experiment was performed in a single-ended *Q*-machine plasma with a specially designed segmented hot end plate. This consisted essentially of two concentric tantalum sections, insulated from each other and separated by an annular nonemitting region. The entire end-plate assembly was heated by electron bombardment. Controlled $E\hat{r} \times B\hat{z}$ velocities in the annular region were established by applying a static voltage between the concentric plate sections. Typical radial profiles of the equilibrium floating potential are shown in Fig. 1(a). These potential distributions can be represented by $\varphi = \varphi_0 \tanh[A \times (r - r_0)]$; here, $A = 7.0 \text{ cm}^{-1}$ and $r_0 = 1.1 \text{ cm}$. The corresponding radial variation of $\vec{E} \times \vec{B}$ rotation frequency is shown in Fig. 1(b), where

$$\omega_E(r) = -mcE(r)/rB, \quad (1)$$

and m is the mode number. We define L as the width of the velocity shear layer.

When the applied voltage is sufficiently large (the value depends on B , k_{\parallel} , n , and dn/dr), oscillations localized in the gap region and traveling in the $\vec{E} \times \vec{B}$ direction are observed. In these experiments, using a potassium plasma, there are as many as seven ion gyroradii in L ,

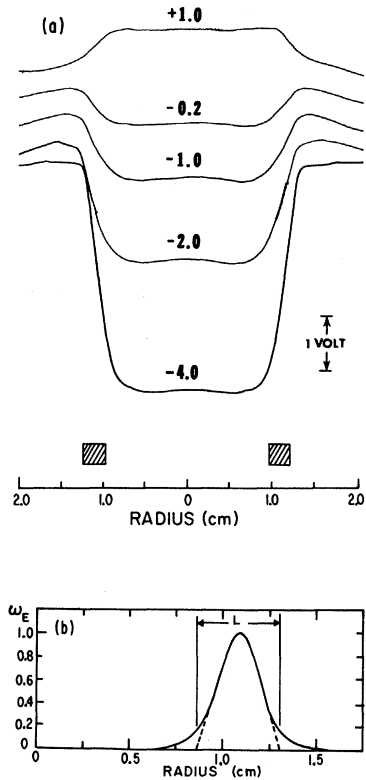


FIG. 1. (a) Radial profiles of floating potential for the segmented end plate for $B=3.2$ kG and $n=4 \times 10^9$ cm^{-3} . There is little change in these profiles over the ranges of B and n in these experiments. Shaded areas show radial extent of the gap between the concentric plate sections. The number on each curve is voltage applied between inner and outer sections. (b) Radial variation of $\vec{E} \times \vec{B}$ rotation frequency. The velocity shear layer is somewhat wider than the gap width (0.24 cm).

so that the finite-Larmor-radius (FLR) fluid equations may be used with confidence, at least for small rotation velocity.⁴ The radial wave equation that describes the normal modes for the Kelvin-Helmholtz (KH) instability in small electric fields has been presented earlier.² The observed instability was identified as the KH type by comparing onset conditions, oscillation frequencies, and radial profiles with the solutions of the radial wave equation together with the electron fluid equations.⁵

Figure 2 shows how the instability evolves when the electric field, directed inward, is increased at constant magnetic field (3.8 kG). The displayed signal is the floating potential oscillation at $r=r_0$. Mode numbers were identified with an azimuthally traveling Langmuir probe. At $E=0$ the plasma is stable and critical (i.e., enhanced thermal) fluctuations are observed.⁶

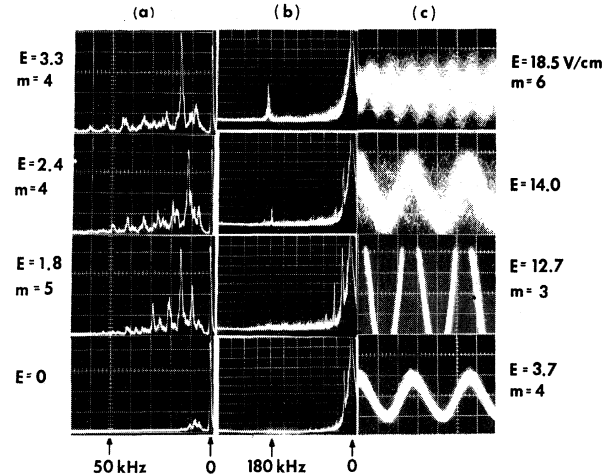


FIG. 2. Mode evolution with electric field E . Here, $B=3.84$ kG and $n=5 \times 10^9$ cm^{-3} . (a) Frequency spectra of potential fluctuation $\tilde{\phi}$ at small electric field, directed inward. Units of E are V/cm. Range of the logarithmic vertical scale is 7 dB/cm. (b) Frequency spectra of $\tilde{\phi}$ at large E , denoted by values on the right. Range of the logarithmic scale is approximately 5 dB/cm. $\omega_c=151$ kHz. (c) Oscilloscope display of $\tilde{\phi}$ for same conditions as (b). Vertical scale is 100 mV/cm and horizontal scale is 20 $\mu\text{sec/cm}$, except for $E=18.5$ V/cm (20 mV/cm and 5 $\mu\text{sec/cm}$).

These are present until instability onset at $E=1.3$ V/cm, where the oscillation amplitude increases by 16 dB. At $E=1.8$ V/cm there is a discrete multimode spectrum peaked at $m=5$ (whose second harmonic obscures $m=8$). At $E=3.3$ V/cm the transition to the single-mode regime occurs, with $m=4$ dominant. A mode switch to $m=3$ follows. Just below $E=14.0$ V/cm this mode begins to damp, and at 14.0 V/cm it has lost 10 dB of its maximum amplitude. Oscillations at 180 kHz ($1.2\omega_c$) appear at this field. At slightly larger E , the $m=3$ KH mode completely disappears, and at $E=18.5$ V/cm, only the $m=6$ oscillation near ω_c is observed. We shall refer to the oscillations at $\omega \gtrsim \omega_c$ as cyclotron waves.

The ion rotation frequency Ω_E includes the polarization drift caused by the changing direction of E :

$$\frac{\Omega_E}{m} = \frac{V_E}{r} = \frac{1}{2}\omega_c \left[-1 + \left(1 + \frac{4}{m} \frac{\omega_E}{\omega_c} \right)^{1/2} \right]. \quad (2)$$

In calculating Ω_{EM} for each transition, where Ω_{EM} is the maximum value of $\Omega_E(r)$, the maximum electric field is the average over the ion orbits at $r=r_0$.

Many mode sequences have been studied. Figure 3(a) shows the normalized Doppler-shifted wave frequency, for the central layer of ions

($r=r_0$), at the electric field at which the final KH mode ($m=2, 3$, or 4) has decreased in amplitude by 10 to 15 dB and cyclotron waves have appeared. The KH mode is usually completely quenched at a slightly larger field. Evidently suppression occurs, at a given magnetic field, when the Doppler-shifted KH frequency lies between $(0.5$ and $0.65)\omega_c$. There was no dependence on n , dn/dr , or k_{\parallel} . Note that $\Omega_{EM} > \omega_r$.

Now consider the multimode spectrum at small E . At large B , the observed dominant KH mode number is $m=6$ or 7 . The theoretical value⁵ is $m=7$ or 8 , and can be calculated simply by defining an effective $k_r=k_0$ and finding the "resonant" mode, $m=\pi r_0/L$. This spectrum is analogous to the hydrodynamic KH spectrum.^{7,8} When B is lowered, FLR stabilization reduces the growth rates of the larger mode numbers, so that at $B=3.8$ kG the dominant mode is $m=5$ [Fig. 2(a)]. For all observed mode sequences, when $V_{EM} \geq 0.6V_T$, there is a series of strong single modes, with successively decreasing mode number. Here, V_T is the ion transverse thermal velocity and V_{EM} the ion azimuthal velocity at $r=r_0$.

The low-frequency theory that neglects the zero-order ion polarization drift is not valid when $V_{EM} > V_T$. Consequently, we have derived a second radial wave equation from the fluid equations in which the zero-order ion polarization drift (due to ion inertia) is retained from the start. We also drop any restriction on the magnitude of ω/ω_c . The ion temperature is neglected, however, since in the large rotation regime $\Omega_{EM} > 20\omega_D$ and FLR stabilization is not important. Also, we set $k_{\parallel}=0$, since parallel resistive motion is relatively unimportant at large rotation velocities.⁹

The dependent variable is the potential fluctuation

$$\bar{\varphi} = \bar{\varphi}(r) \exp(im\theta - i\omega t), \quad (3)$$

and the result is

$$\frac{d^2 \bar{\varphi}}{dr^2} + \frac{d\bar{\varphi}}{dr} \left\{ \frac{1}{n} \frac{dn}{dr} + \frac{1}{r} - \frac{1}{A_5} \frac{dA_5}{dr} \right\} + \bar{\varphi} \left\{ -\frac{m}{r} \frac{1}{n} \frac{dn}{dr} \frac{A_5}{A_4 \omega_c} - \left(\frac{m}{r} \right)^2 - \frac{1}{n} \frac{dn}{dr} \frac{m A_2}{r A_1} - \frac{m}{r} \frac{1}{A_1} \frac{dA_2}{dr} + \frac{m}{r} \frac{A_2}{A_1 A_5} \frac{dA_5}{dr} \right\} = 0, \quad (4)$$

where

$$A_1 = \omega - \Omega_E, \quad A_2 = 2 \left(\frac{\Omega_E}{m} \right) + \omega_c, \quad A_3 = \omega_c + 2 \frac{\Omega_E}{m} + \frac{r}{m} \frac{d\Omega_E}{dr}, \quad A_4 = \omega - \omega_E, \quad A_5 = A_1^2 - A_2 A_3. \quad (5)$$

If we set $\omega_E = \Omega_E$, multiply through by $A_1 = A_4$, and retain terms up to first order in ω/ω_c and ω_E/ω_c , we recover Eq. (3.15) of Rosenbluth and Simon⁹ with zero ion temperature.

Solutions to Eq. (4) were found by numerical integration, with $\omega_E = (1/r) \operatorname{sech}^2[7(r-1.1)]$. Figure 3(b)

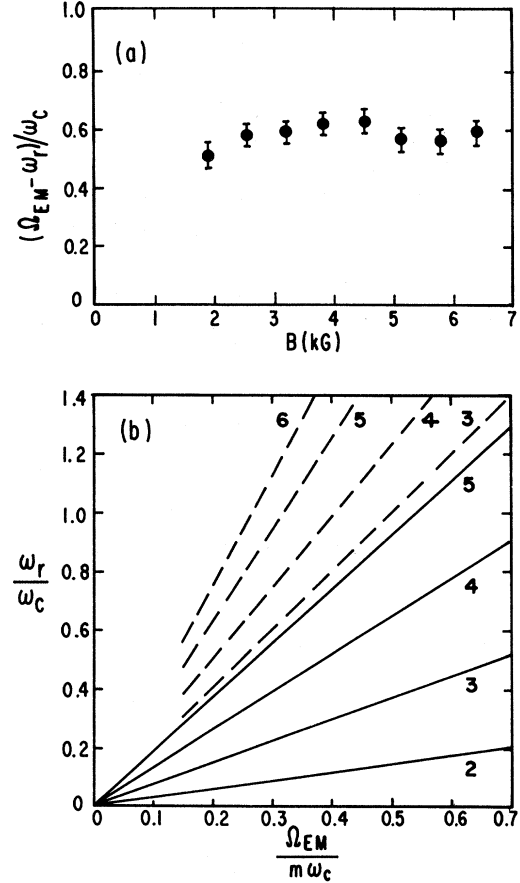


FIG. 3. (a) Doppler-shifted oscillation frequency of the final Kelvin-Helmholtz mode at suppression, as a function of magnetic field. Vertical bars represent rms deviations for many mode sequences under various conditions of n , dn/dr , and hot end-plate temperature. The quantity Ω_{EM} is calculated using the average electric field over the orbits of ions whose guiding centers are located at the maximum electric field. (b) Oscillation frequencies for the unstable solutions of Eq. (4), with $n'/(nr) = -1.0 \text{ cm}^{-2}$. Solid lines are the type-A, low-frequency Kelvin-Helmholtz solutions. Dashed lines are the type-B solutions. Numbers designate the modes.

shows that for each mode number there are two unstable solutions in the range $\omega \lesssim \omega_c$. The type-A solutions at the lower frequencies are the KH waves. The type-B solutions have frequencies several times larger. The growth rate of these modes depends only weakly on mode number, and is always less than the growth rate of any type-A mode ($m > 1$). All of these instabilities are localized in the velocity shear layer. The type-B solutions have properties in good agreement with the frequencies, mode numbers, and localization of the observed cyclotron waves. For example, the $m=6$ mode in Fig. 2(b) at $E = 18.5$ V/cm ($\Omega_{EM}/m\omega_c = 0.35$) has $\omega_r = 1.25\omega_c$, compared with the theoretical value of $1.3\omega_c$ from Fig. 3(b). Experimentally, as E is increased there is mode switching in such a fashion that ω is always $(1.0$ to $1.4)\omega_c$. At electric fields below the suppression value, the critical fluctuations⁶ for these modes were observed at $\omega \lesssim \omega_c$. Note that the observed oscillations cannot be electrostatic ion cyclotron waves, because previous investigations of these waves have shown $m=0$, which disagrees with the large mode numbers measured here.

Finally, we consider the large electric-field suppression of the KH modes. Figure 3(a) shows that there is an empirical maximum electric field at which KH modes may exist. The suppression phenomenon is independent of density, at least in the range $1 \times 10^9 < n < 3 \times 10^{10}$ cm⁻³, and independent of dn/dr . One explanation consistent with the experimental results is nonlinear Landau damping,³ in which the KH wave interacts nonlinearly with itself and with the gyrating ions. The resonant condition for nonlinear Landau damping in a magnetic field with $k_{\parallel} = 0$ (in the experiment, $k_{\parallel} V_T \sim 10^{-3}\omega_c$), when the wave interacts with itself,³ is

$$\Omega_{EM} - \omega = \frac{1}{2} \omega_c. \quad (6)$$

Actually this condition, which is close to the experimental stabilization condition, need be met only to within the linear relaxation rate. This nonlinear damping mechanism cannot be responsible for total suppression, but it can reduce the effective growth rate to zero, so the cyclotron wave may displace it.¹⁰

In conclusion, the evolution of the Kelvin-

Helmholtz instability driven by shear in the $\vec{E} \times \vec{B}$ rotation develops from the stable plasma with critical fluctuations to threshold, followed by the hydrodynamic multimode spectrum, then a succession of strong single modes, and, finally, complete suppression when the Doppler-shifted wave frequency for the central layer of ions is $(0.50$ to $0.65)\omega_c$. The cyclotron waves observed upon low-frequency suppression have properties in agreement with the solutions of the fluid equations for large nonuniform rotation.

The author is grateful to Dr. H. W. Hendel, Dr. R. W. Motley, Dr. F. W. Perkins, and Mr. R. L. Dewar for valuable discussions. Dr. Alfred Y. Wong suggested the search for cyclotron waves. This work was performed under the auspices of the U. S. Atomic Energy Commission under Contract No. AT(30-1)-1238.

*Present address: Electrical Sciences and Engineering Department, University of California, Los Angeles, Calif. 90024.

¹G. I. Kent, N. C. Jen, and F. F. Chen, *Phys. Fluids* **12**, 2140 (1969).

²D. L. Jassby and F. W. Perkins, *Phys. Rev. Lett.* **24**, 256 (1970).

³M. N. Rosenbluth, B. Coppi, and R. N. Sudan, *Ann. Phys. (New York)* **55**, 248 (1969).

⁴A similar experimental arrangement, but using an end plate heated by radiation from a surrounding cylinder, was achieved by L. Enriques, A. M. Levine, and G. B. Righetti and reported in *Proceedings of the Third International Conference on Plasma Physics and Controlled Nuclear Fusion Research Novosibirsk, U.S.S.R., 1968* (International Atomic Energy Agency, Vienna, Austria, 1969), Vol. I, p. 641. They observed oscillations localized in the gap region, but gave no theory. In their experiments the ion gyroradius was comparable to the width of the shear layer.

⁵D. L. Jassby and R. W. Motley, *Bull. Amer. Phys. Soc.* **15**, 508 (1970). A detailed report on the instability identification will be published.

⁶H. W. Hendel and T. K. Chu, in "Methods of Experimental Physics," edited by H. Griem (Academic, New York, to be published) Vol. 9A, Chap. 9.

⁷P. G. Drazin and L. N. Howard, *J. Fluid Mech.* **14**, 257 (1963).

⁸F. W. Perkins and D. L. Jassby, to be published.

⁹M. N. Rosenbluth and A. Simon, *Phys. Fluids* **8**, 1300 (1965).

¹⁰T. H. Dupree, *Phys. Fluids* **11**, 2680 (1968).

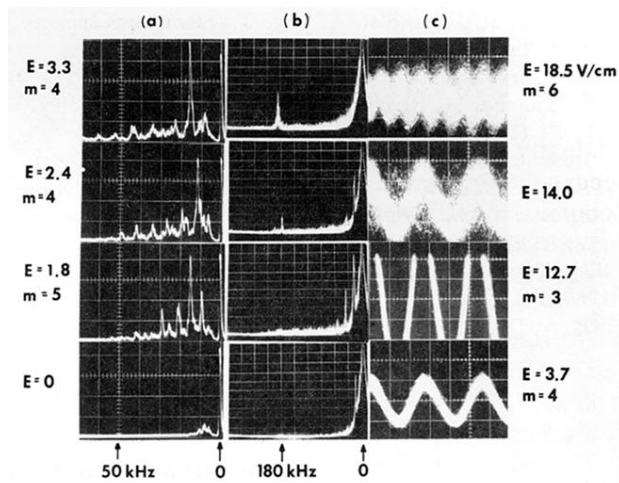


FIG. 2. Mode evolution with electric field E . Here, $B = 3.84$ kG and $n = 5 \times 10^9$ cm $^{-3}$. (a) Frequency spectra of potential fluctuation $\tilde{\varphi}$ at small electric field, directed inward. Units of E are V/cm. Range of the logarithmic vertical scale is 7 dB/cm. (b) Frequency spectra of $\tilde{\varphi}$ at large E , denoted by values on the right. Range of the logarithmic scale is approximately 5 dB/cm. $\omega_c = 151$ kHz. (c) Oscilloscope display of $\tilde{\varphi}$ for same conditions as (b). Vertical scale is 100 mV/cm and horizontal scale is 20 μ sec/cm, except for $E = 18.5$ V/cm (20 mV/cm and 5 μ sec/cm).